PLOS ONE

RESEARCH ARTICLE

Effect of linker on the binding free energy of stapled p53/HDM2 complex

Haeri Im, Sihyun Ham*

Department of Chemistry, The Research Institute of Natural Sciences, Sookmyung Women's University, Seoul, Korea

* sihyun@sookmyung.ac.kr

OPEN ACCESS

Citation: Im H, Ham S (2020) Effect of linker on the binding free energy of stapled p53/HDM2 complex. PLoS ONE 15(4): e0232613. https://doi.org/10.1371/journal.pone.0232613

Editor: Claudio M. Soares, Universidade Nova de Lisboa Instituto de Tecnologia Quimica e Biologica, PORTUGAL

Received: December 30, 2019

Accepted: April 18, 2020

Published: April 30, 2020

Peer Review History: PLOS recognizes the benefits of transparency in the peer review process; therefore, we enable the publication of all of the content of peer review and author responses alongside final, published articles. The editorial history of this article is available here: https://doi.org/10.1371/journal.pone.0232613

Data Availability Statement: All relevant data are within the manuscript and its Supporting Information files.

Funding: This study was funded by the Samsung Science and Technology Foundation under Project

Abstract

Inactivation of the tumor suppressor p53 resulting from the binding with a negative regulator HDM2 is among the predominant defects in human cancers. p53-mimicking peptides whose conformational and proteolytic stability is enhanced by an all-hydrocarbon staple are being recognized as promising anticancer agents for disrupting the p53–HDM2 binding and reactivating p53. Herein, we conduct a computational modeling and thermodynamic characterization of stapled p53/HDM2 complex via molecular docking, simulations, and binding free energy analysis. The binding thermodynamics analysis is done based on the end-point calculation of the effective binding energy—a sum of the direct peptide–protein interaction energy and the dehydration penalty—and on its decomposition into contributions from specific groups constituting the complex. This allows us to investigate how individual amino acids in the stapled p53 and HDM2 contribute to the binding affinity. We find that not only the epitope residues (F19, W23 and L26), but also the hydrocarbon linker of the stapled p53 impart significant contributions. Our computational approach will be useful in designing new stapled peptides in which the staple location is also optimized to improve the binding affinity.

Introduction

The p53 protein is a transcription factor regulating cell cycle and apoptosis in response to DNA damages and cellular stresses [1]. It plays a critical role for maintaining the genome integrity and preventing the development of tumor [2]. The p53 levels in normal cells are controlled by negative regulator proteins such as HDM2 that neutralize the p53 transactivation activity via a direct binding interaction [3]. The loss of p53 activity resulting from the binding with overexpressed HDM2 is among the predominant defects in human cancers [4]. The reactivation of p53 by perturbing the p53–HDM2 binding has therefore been regarded as a promising approach for suppressing tumor growth in cancer cells [5–7].

The p53–HDM2 interaction occurs primarily between the short α-helical segment of p53 and the hydrophobic pocket of the HDM2 surface. In particular, three residues (F19, W23 and L26) within this segment form critical contacts with HDM2 [8]. p53-mimicking peptides incorporating these epitope residues will hence serve as potential anticancer agents that reactivate p53 by driving it out from the interaction with HDM2. In this context, there is recently a

Number SSTF-BA1401-52 and the National Research Foundation of Korea (NRF) (No. NRF-2017R1A2B3010053) to SH. The funders had no role in study design, data collection and analysis, decision to publish, or preparation of the manuscript.

Competing interests: The authors have declared that no competing interests exist.

growing interest in stapled peptides in which an α-helical conformation appropriate to binding with HDM2 is rigidified through an introduction of an all-hydrocarbon linkage connecting helix forming residues [9–13]. Furthermore, it has been demonstrated that the stapling also enhances the proteolytic stability and promotes cell permeability, which are crucial for *in vivo* therapeutic activity [14]. Systematic mutational analysis, including the optimization of the staple locations, are being carried out experimentally and computationally in search of higher binding affinity and more improved potency and specificity [15,16].

Herein, we propose a computational method that is useful for designing new stapled p53-mimicking peptides (to be simply referred to as stapled p53 peptides from here on). We start from a peptide sequence and conduct a template-based modeling using an experimental structure. The stapled p53 peptide so constructed is subjected to molecular dynamics simulations to explore a representative structure in an aqueous solution and its conformational stability. The simulated stapled p53 structure is then used for a molecular docking onto the HDM2 surface. Starting from the docked complex structure, we perform molecular dynamics simulations. For the simulated complex configurations, we finally carry out thermodynamic analysis. This is done based on the end-point calculation of the effective binding free energy Δf [17]. It comprises the direct peptide-protein interaction energy (ΔE_u) and the solvation free energy contribution (ΔG_{solv}), $\Delta f = \Delta E_u + \Delta G_{solv}$. The quantity Δf is connected to the binding free energy (ΔG_{bind}) via $\Delta G_{bind} = \Delta f - T(\Delta S_{config} + \Delta S_{ext})$ in which ΔS_{config} and ΔS_{ext} are the configurational and external entropies, respectively [18,19]. Since these entropy terms are typically negative, the favorable contributions to the binding affinity arise mainly from Δf. The formation of peptide–protein contacts, such as hydrogen bonds and van der Waals contacts, leads to favorable changes in the direct interaction energy ($\Delta E_u < 0$). However, the formation of these peptide–protein contacts involves the dehydration penalty ($\Delta G_{solv} > 0$). Therefore, in arguing the net contribution to the binding affinity, it is essential to analyze Δf that simultaneously takes into account both ΔE_u and ΔG_{solv}. Importantly, Δf can be decomposed into contributions from specific groups constituting the complex [20,21]. Thereby, our method allows us not only to investigate the relevance of individual amino acids, but also to quantify the contribution from the hydrocarbon linker to the binding affinity.

Materials and methods

Modeling stapled p53/HDM2 complex

We investigated a stapled p53 peptide, referred to as sMTide-02 in Ref. [14], whose sequence is Ac-TSFXEYWALLX-NH2 (X: linker positions): two additional peptides stapled at shifted positions, Ac-TXFAEYWAXLS-NH2 (to be referred to as sMTide-02b) and Ac-XSFAEYWXLLS-NH2 (sMTide-02c) were also studied to analyze the dependence of the structural stability and binding affinity on the linker location (see Fig 1A). Each peptide structure was constructed using an experimental structure for a stapled p53 (PDB ID 3V3B) [15] as a template. The hydrocarbon linker was added with GaussView [22]. A 100 ns molecular dynamics simulation was carried out for each stapled peptide starting from the constructed structure (see below for details on the simulation). A representative peptide conformation for each system was selected based on the *k*-means clustering with a radius of 4.0 Å (shown in Fig 1A), which was then used in the docking onto the HDM2 surface. We employed the X-ray structure (PDB ID 1YCR) [8] for HDM2 (Fig 1B). The docking was performed using AutoDock Vina [23]. Only the side chains were permitted to rate in the docking simulation. 1,000 complex structures were generated from the docking carried out for each system, and we chose the most stable structure. Molecular dynamics simulations for the stapled p53/HDM2 complexes were then carried out starting from the respective docked structures.

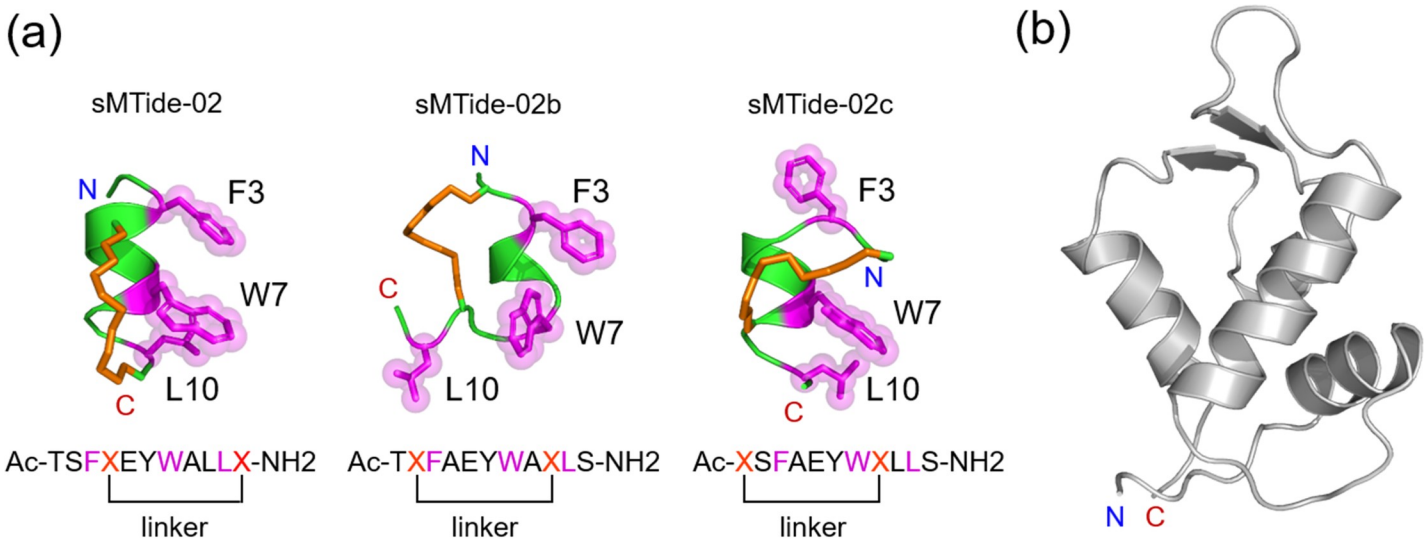

Fig 1. Stapled p53 peptide and HDM2 structures. (a) Simulated stapled p53 peptides (sMTide-02, sMTide-02b and sMTide-02c). Three epitope residues (F3, W7, and L10; colored magenta) and the hydrocarbon linker (colored orange) are indicated by stick representations. (b) X-ray structure for HDM2 (PDB ID 1YCR).

https://doi.org/10.1371/journal.pone.0232613.g001

Molecular dynamics simulations

Simulations for the free stapled p53 peptides and the stapled p53/HDM2 complexes were carried out using AMBER16 [24]. Each system was solvated by waters and counter ions. The ff99SB-ILDN [25,26] was adopted for the peptide/protein and for water the TIP3P model [27] was used. The linker partial charges were determined from the restrained electrostatic potential (RESP) method [28] after carrying out an HF/6-31G* quantum mechanical calculation with Gaussian 09 [29]. We employed the general Amber force field [30] for the other parameters. After the standard minimization and equilibration steps, 100 ns *NPT*-ensemble simulations were performed at 300 K and 1 bar. A single and 10 independent runs were conducted for the free peptide and the complex, respectively.

Thermodynamic calculations

The effective binding free energy, $\Delta f = \Delta E_u + \Delta G_{solv}$, was computed using the simulated complex structures saved with a 1 ns interval. The direct peptide-protein interaction energy (ΔE_u) can be obtained easily from the force field parameters. The solvation term (ΔG_{solv}) comprises the ones for the complex and its components, $\Delta G_{solv} = G_{solv;\ complex} - (G_{solv;\ stapled\ p53} + G_{solv;\ HDM2})$, and was computed using the 3D-RISM theory [31,32].

Within the classical force field, the direct interaction energy (ΔE_u) is expressed as a sum of atomic contributions. For the solvation free energy (G_{solv}), we have recently developed an exact atomic decomposition method [20,21]. Thereby, the effective binding free energy (Δf) can be partitioned into contributions from constituent atoms. By an appropriate grouping of these atomic terms, individual residue and linker contributions to Δf can be obtained.

Results and discussion

We first performed a 100 ns free-peptide simulation for each of the stapled p53 peptides (sMTide-02, sMTide-02b and sMTide-02c) to examine its conformational stability in an aqueous environment. The free sMTide-02 was quite stable (the Cα root-mean-squared deviation (RMSD) to the initial structure remained <1.0 Å) during the simulation. Its overall helical

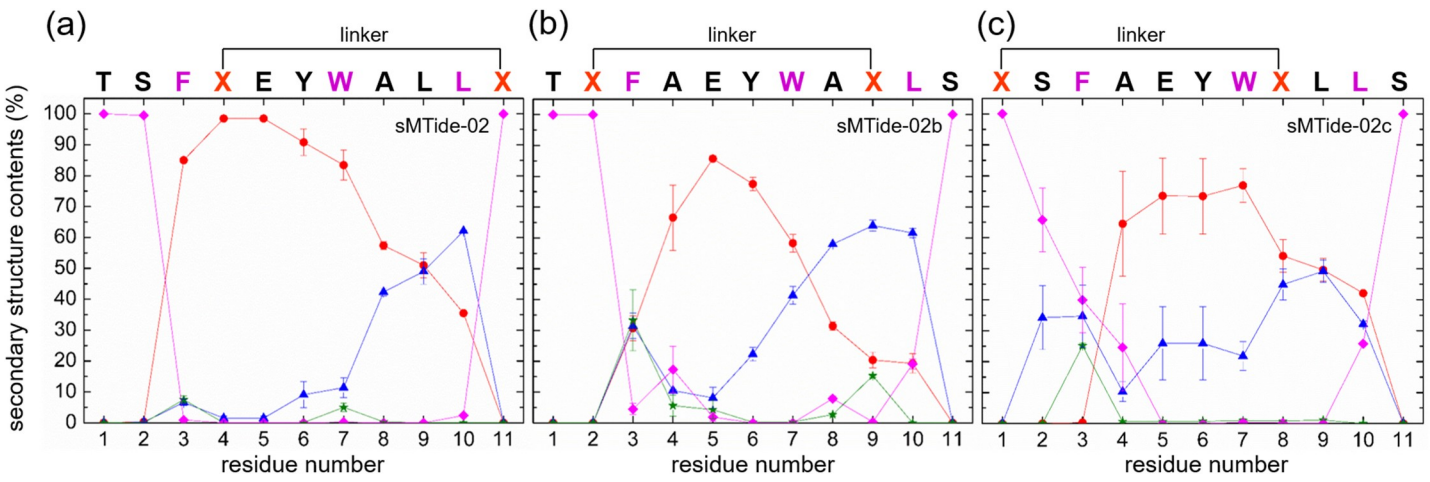

Fig 2. Average secondary structure contents of the free stapled p53 peptides. (a–c) Average secondary structure contents for the free sMTide-02 (a), sMTide-02b (b) and sMTide-02c (c) (red circles, helix; blue triangles, turn; green stars, bend, and magenta diamonds, coil).

https://doi.org/10.1371/journal.pone.0232613.g002

structure was also maintained (Fig 2A) with an average helical content of 55%. It is well known that short helical segments taken out from globular proteins cannot keep up its secondary structure when isolated [33]. Our simulation thus confirms the significantly enhanced conformational stability of a short helical peptide brought about by the staple linker. On the other hand, the structures of the other stapled peptides (sMTide-02b and sMTide-02c) exhibited somewhat larger deviations: the Cα RMSDs to the respective initial structures increased up to 1.6 Å and 2.4 Å and the average helical contents dropped to 35% (Fig 2B) and 39% (Fig 2C), respectively. Thus, the stability and helicity of the stapled p53 peptides depend on the linker positions.

We next performed 10 independent 100 ns molecular dynamics simulations for the stapled p53/HDM2 complex (formed with each of sMTide-02, sMTide-02b and sMTide-02c) after docking the simulated free stapled p53 peptide onto the HDM2 surface. Representative complex structures therefrom are displayed in Fig 3. In the wild-type p53/HDM2 complex, the epitope residues (F19, W23 and L26) enter deep inside the HDM2 hydrophobic pocket (comprising M26, L30, L33, G34, I37, M38, Y43, H49, V51, F67, V69, H72, I75 and Y76). Such an interface topology is well conserved in the simulated sMTide-02/HDM2 complex; the epitope residues (F3, W7 and L10) of sMTide-02 make hydrophobic contacts with most of the HDM2 residues listed above (L30, F31, L33, G34, I37, M38, Y43, V51, V69, H72, and I75). We also find that the hydrocarbon linker (colored orange) makes contacts with the hydrophobic residues (F31, G34, and M38) in the HDM2 binding surface (colored yellow). Such an interaction between the peptide staple and protein has been observed in previous simulation studies for the related systems [34,35]. For the complexes formed with the stapled p53 peptides in which the linker positions are shifted (sMTide-02b and MTide-02c), we find that the binding of the epitope residues and the linker to HDM2 is not so prominent and involves less contacts with HDM2 (sMTide-02b contacts only with L30, F31, L33, F34, I37, M38, Y43, V69, I75, whereas sMTide-02c with L30, F31, L33, I37, M38, F67, H72, I75). This indicates that the less helical structures of these stapled p53 peptides are not optimal in binding to HDM2.

Finally, we conducted the end-point calculations of the effective binding free energy (Δf) based on the simulated complex structures. As we stated above, Δf provides the major favorable contribution to the binding affinity. Therefore, its decomposition into specific group contributions enables us to identify critical residues. The effective binding free energies for HDM2

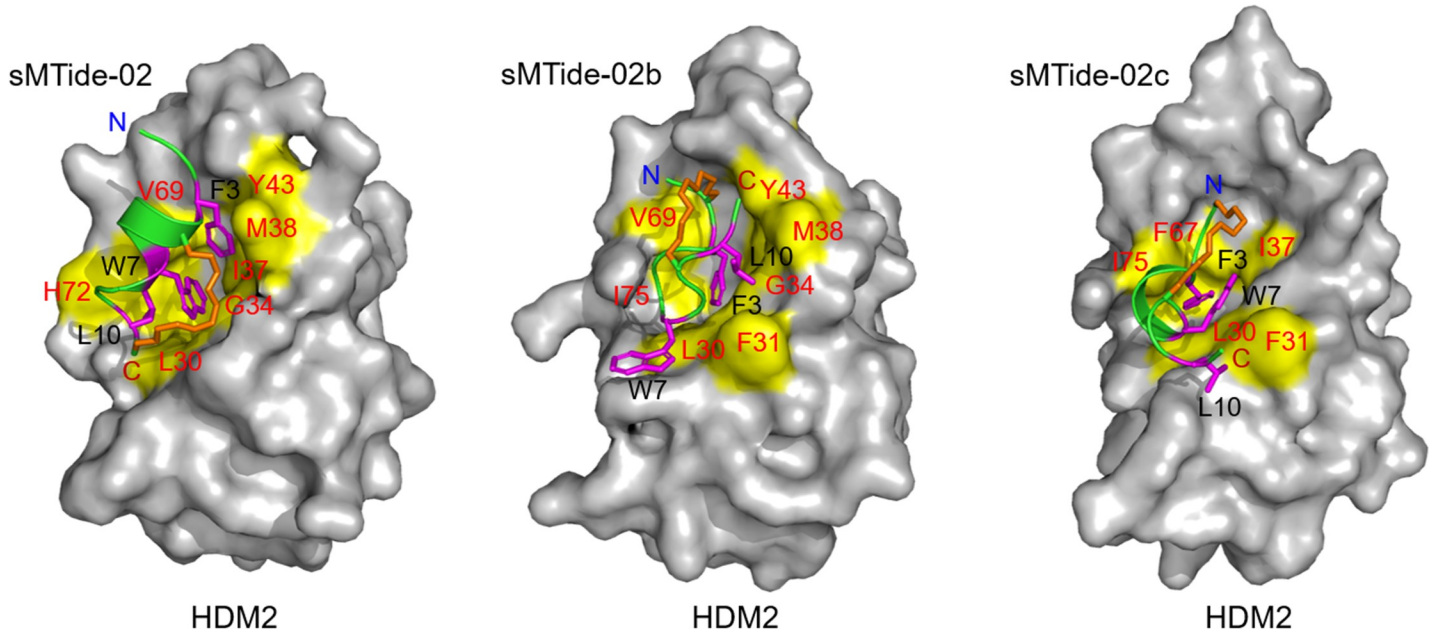

Fig 3. Representative structures of simulated stapled p53/HDM2 complexes. Three epitope residues (F3, W7, and L10; colored magenta) of the stapled p53 peptides are indicated by stick representations. The yellow surface shows the hydrophobic surface (comprising the residues colored red) of HDM2 interacting with the epitope residues.

https://doi.org/10.1371/journal.pone.0232613.g003

with sMTide-02, sMTide-02b and sMTide-02c were computed to be –18.7 ± 0.5 kcal/mol, –13.2 ± 1.0 kcal/mol, and –7.0 ± 0.8 kcal/mol, respectively (average ± standard error estimated from the respective 10 independent runs). This trend is in accord with the experimental observation for the related SAH-p53 (stabilized alpha-helix of p53) peptides [9]: The linker positions in sMTide-02, sMTide-02b and sMTide-02c corresponds to those in SAH-p53-8, SAH-p53-2 and SHA-p53-3 peptides, respectively, whose binding affinities for HDM2 decrease in this order. The decomposition of the effective binding energy into constituent amino acids is shown in Fig 4. We find that the epitope residues (F3, W7 and L10; colored magenta) of the stapled peptides and the hydrophobic residues located at the HDM2 binding surface (colored yellow) are in fact the principal contributors to the binding affinity. Interestingly, we observe that the hydrocarbon linker of sMTide-02 (colored orange) also provides a significant contribution. In this regard, we emphasize the more relevance of analyzing Δf than just examining the direct peptide–protein interaction energy (ΔE_u). Indeed, as can be inferred from S1 Fig that further partitions Δf into ΔE_u and ΔG_{solv} terms, the contributions from the epitope residues and the hydrocarbon linker to ΔE_u are comparable to those from the other residues in the stapled peptide, and hence, their significance cannot be elucidated solely in terms of ΔE_u. Only after taking into account the dehydration penalty embodied in ΔG_{solv}, the special role of the epitope residues and the hydrocarbon linker becomes evident. This demonstrates the essential importance of analyzing Δf in identifying the residues critical to binding. The significant contributions from the hydrocarbon linker is also observable in sMTide-02b and sMTide-02c, albeit to a lesser extent. (The partitioning of Δf into ΔE_u and ΔG_{solv} for sMTide-02b and sMTide-02c is presented in S2 and S3 Figs, respectively.) Correspondingly, the contributions from the epitope residues of sMTide-02b and sMTide-02c are somewhat smaller than those of sMTide-02. This indicates that, in designing stapled peptides, the location of the linker should be optimized also from the standpoint of binding affinity.

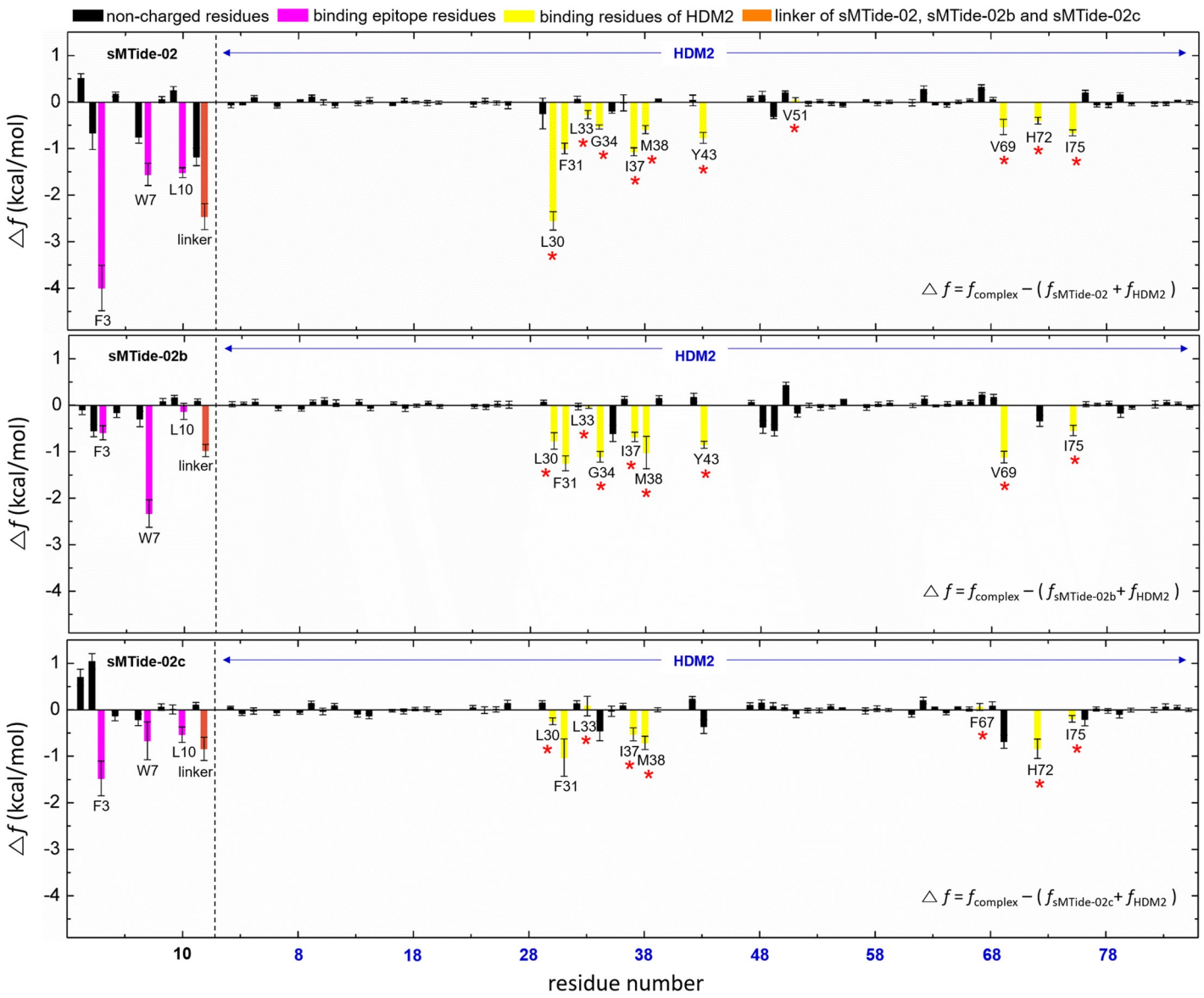

Fig 4. Analysis of the effective binding free energy (Δ*f*). The epitope residues of the stapled p53 peptides are colored magenta and the hydrocarbon linker is colored orange; hydrophobic residues located at the binding interface of HDM2 are colored yellow; and residues present in the wild-type p53/HDM2 binding interface are indicated by the red stars.

https://doi.org/10.1371/journal.pone.0232613.g004

Conclusions

We present a computational method for modeling and characterizing stapled peptides and illustrate its application to a stapled p53/HDM2 complex. Putative initial structures for the free stapled p53 peptides and their complexes with HDM2 are generated by a template-based modeling and docking tools, which are subsequently validated via molecular dynamics simulations in an aqueous environment. Thermodynamic characterization of the stapled p53/HDM2 complex is done by decomposing the effective binding free energy into specific constituent groups. This method allows one to identify hot spot residues critical to binding. In fact, we identify the epitope residues of the stapled p53 and the hydrophobic residues of the HDM2 surface to be the principal contributors to the binding affinity. We also find that the

hydrocarbon linker of the stapled p53 provides a significant contribution. Thus, the linker plays an important role not only in stabilizing the helical peptide appropriate to binding, but also in determining the binding thermodynamics. Our method will be useful in designing new stapled peptides in which the staple location can be optimized from the thermodynamic viewpoint.

Supporting information

S1 Fig. Further partitioning of the residue-decomposed effective binding energy Δf into the ΔE_u and ΔG_{solv} terms for the complex with sMTide-02.
(TIF)

S2 Fig. Further partitioning of the residue-decomposed effective binding energy Δf into the ΔE_u and ΔG_{solv} terms for the complex with sMTide-02b.
(TIF)

S3 Fig. Further partitioning of the residue-decomposed effective binding energy Δf into the ΔE_u and ΔG_{solv} terms for the complex with sMTide-02c.
(TIF)

Author Contributions

Conceptualization: Sihyun Ham.

Data curation: Haeri Im, Sihyun Ham.

Formal analysis: Haeri Im, Sihyun Ham.

Funding acquisition: Sihyun Ham.

Investigation: Haeri Im, Sihyun Ham.

Methodology: Haeri Im, Sihyun Ham.

Project administration: Sihyun Ham.

Resources: Sihyun Ham.

Software: Sihyun Ham.

Supervision: Sihyun Ham.

Validation: Sihyun Ham.

Visualization: Haeri Im, Sihyun Ham.

Writing – original draft: Haeri Im, Sihyun Ham.

Writing – review & editing: Haeri Im, Sihyun Ham.

References

1. Walker KK, Levine AJ. Identification of a novel p53 functional domain that is necessary for efficient growth suppression. Proc Natl Acad Sci USA. 1996; 93(26): 15335–15340. doi:doi: 10.1073/pnas.93.26.15335 PMID: 8986812
2. Efeyan A, Serrano M. p53: Guardian of the genome and policeman of the oncogenes. Cell Cycle. 2007; 6(9): 1006–1010. doi:doi: 10.4161/cc.6.9.4211 PMID: 17457049
3. Vousden KH, Lane DP. p53 in health and disease. Nat Rev Mol Cell Biol. 2007; 8: 275–283. doi:doi: 10.1038/nrm2147 PMID: 17380161

4. Khoo KH, Verma CS, Lane DP. Drugging the p53 pathway: understanding the route to clinical efficacy. Nat Rev Drug Discov. 2014; 13: 217–236. doi:doi: 10.1038/nrd4236 PMID: 24577402

5. Honda R, Tanaka H, Yasuda H. Oncoprotein MDM2 is a ubiquitin ligase E3 for tumor suppressor p53. FEBS Lett. 1997; 420: 25–27. https://doi.org/10.1016/s0014-5793(97)01480-4 PMID: 9450543

6. Onel K, Cordon-Cardo C. MDM2 and prognosis. Mol Cancer Res. 2004; 2: 1–8. https://mcr.aacrjournals.org/content/2/1/1.short PMID: 14757840

7. Wanzel M, Vischedyk JB, Gittler MP, Gremke N, Seiz JR, Hefter M, et al. CRISPR-Cas9-based target validation for p53-reactivating model compounds. Nat Chem Biol. 2016; 12(1): 22–28. https://doi.org/10.1038/nchembio.1965

8. Kussie PH, Gorina S, Marechal V, Elenbaas B, Moreau J, Levine AJ, et al. Structure of the MDM2 oncoprotein bound to the p53 tumor suppressor transactivation domain. Science. 1996; 274(5289): 948–953. doi:doi: 10.1126/science.274.5289.948 PMID: 8875929

9. Bernal F, Tyler AF, Korsmeyer SJ, Walensky LD, Verdine GL. Reactivation of the p53 tumor suppressor pathway by a stapled p53 peptide. J Am Chem Soc. 2007; 129(9): 2456–2457. doi:doi: 10.1021/ja0693587 PMID: 17284038

10. Zwier MC, Pratt AJ, Adelman JL, Kaus JW, Zuckerman DM, Chong LT. Efficient atomistic simulation of pathways and calculation of rate constants for a protein−peptide binding process: Application to the MDM2 protein and an intrinsically disordered p53 peptide. J Phys Chem Lett. 2016; 7(17): 3440−3445. doi:doi: 10.1021/acs.jpclett.6b01502 PMID: 27532687

11. Paul F, Wehmeyer C, Abualrous ET, Wu H, Crabtree MD, Schöneberg J, et al. Protein-peptide association kinetics beyond the seconds timescale from atomistic simulations. Nat Commun. 2017; 8: 1095. doi:doi: 10.1038/s41467-017-01163-6 PMID: 29062047

12. Morrone JA, Perez A, MacCallum J, Dill KA. Computed binding of peptides to proteins with MELD-accelerated molecular dynamics. J Chem Theory Comput. 2017; 13(2): 870−876. doi:doi: 10.1021/acs.jctc.6b00977 PMID: 28042966

13. Tran DP, Kitao A. Dissociation process of a MDM2/p53 complex investigated by parallel cascade selection molecular dynamics and the markov state model. J Phys Chem B. 2019; 123(11): 2469−2478. doi:doi: 10.1021/acs.jpcb.8b10309 PMID: 30645121

14. Brown CJ, Quah ST, Jong J, Goh AM, Chiam PC, Khoo KH, et al. Stapled peptides with improved potency and specificity that activate p53. ACS Chem Biol. 2013; 8(3): 506–512. doi:doi: 10.1021/cb3005148 PMID: 23214419

15. Baek S, Kutchukian PS, Verdine GL, Huber R, Holak TA, Lee KW, et al. Structure of the stapled p53 peptide bound to Mdm2. J Am Chem Soc. 2012; 134(1): 103–106. doi:doi: 10.1021/ja2090367 PMID: 22148351

16. Chang YS, Graves B, Guerlavais V, Tovar C, Packman K, To KH, et al. Stapled α−helical peptide drug development: A potent dual inhibitor of MDM2 and MDMX for p53-dependent cancer therapy. Proc Natl Acad Sci USA. 2013; 110(36): E3445–E3454. doi:doi: 10.1073/pnas.1303002110 PMID: 23946421

17. Gohlke H, Case DA. Converging Free Energy Estimates: MM-PB(GB)SA studies on the protein–protein complex Ras–Raf. J Comput Chem. 2004; 25(2): 238–250. doi:doi: 10.1002/jcc.10379 PMID: 14648622

18. Gilson MK, Given JA, Bush BL, McCammon JA. The statistical-thermodynamic basis for computation of binding affinities: A critical review. Biophys J. 1997; 72(3): 1047–1069. https://doi.org/10.1016/S0006-3495(97)78756-3 PMID: 9138555

19. Chong SH, Ham S. New computational approach for external entropy in protein−protein binding. J Chem Theory Comput. 2016; 12(6): 2509–2516. doi:doi: 10.1021/acs.jctc.6b00174 PMID: 27153451

20. Chong SH, Ham S. Atomic decomposition of the protein solvation free energy and its application to amyloid-beta protein in water. J Chem Phys. 2011; 135(3): 034506. doi:doi: 10.1063/1.3610550 PMID: 21787012

21. Chong SH, Ham S. Distinct role of hydration water in protein misfolding and aggregation revealed by fluctuating thermodynamics analysis. Acc Chem Res. 2015; 48(4): 956–965. doi:doi: 10.1021/acs.accounts.5b00032 PMID: 25844814

22. Dennington RD, Keith TA, Millam J. GaussView, Version 5, Semichem Inc, Shawnee Mission, KS, USA. 2009.

23. Trott O, Olson AJ. AutoDock Vina: Improving the speed and accuracy of docking with a new scoring function, efficient optimization, and multithreading. J Comput Chem. 2010; 31(2): 455–461. doi:doi: 10.1002/jcc.21334 PMID: 19499576

24. Case DA, Betz RM, Cerutti DS, Cheatham TE, Darden TA, Duke RE, et al. AMBER 2016, University of California, San Francisco.

25. Hornak V, Abel R, Okur A, Strockbine B, Roitberg A, Simmerling C. Comparison of multiple Amber force fields and development of improved protein backbone parameters. Proteins. 2006; 65(3): 712–725. doi:doi: 10.1002/prot.21123 PMID: 16981200

26. Lindorff-Larsen K, Piana S, Palmo K, Maragakis P, Klepeis JL, Dror RO, et al. Improved side-chain torsion potentials for the amber ff99SB protein force field. Proteins. 2010; 78(8): 1950–1958. doi:doi: 10.1002/prot.22711 PMID: 20408171

27. Jorgensen WL, Chandrasekhar J, Madura JD, Impey RW, Klein ML. Comparison of simple potential functions for simulating liquid water. J Chem Phys. 1983; 79(2): 926–935. https://doi.org/10.1063/1.445869

28. Wang J, Cieplak P, Kollman PA. How well does a restrained electrostatic potential (RESP) model perform in calculating conformational energies of organic and biological molecules? J Comput Chem. 2000; 21(12): 1049–1074. https://doi.org/10.1002/1096-987X(200009)21:12<1049::AID-JCC3>3.0.CO;2-F

29. Frisch MJ, Trucks GW, Schlegel HB, Scuseria GE, Robb MA, Cheeseman JR, et al. Gaussian09, Revision E01 Gaussian, Inc, Wallingford CT. 2009.

30. Wang J, Wolf RM, Caldwell JW, Kollman PA, Case DA. Development and testing of a general amber force field. J Comput Chem. 2004; 25(9): 1157–1174. doi:doi: 10.1002/jcc.20035 PMID: 15116359

31. Kovalenko A, in: Molecular Theory of Solvation (Ed.: Hirata F), Kluwer Academic, Dordrecht; 2003. pp. 169.

32. Imai T, Harano Y, Kinoshita M, Kovalenko A, Hirata F. A theoretical analysis on hydration thermodynamics of proteins. J Chem Phys. 2006; 125(2): 024911. https://doi.org/10.1063/1.2213980

33. Dill K. Dominant Forces in Protein Folding. Biochemistry. 1990; 29(31): 7133–7155. doi:doi: 10.1021/bi00483a001 PMID: 2207096

34. Joseph TL, Lane D, Verma CS. Stapled peptides in the p53 pathway: Computer simulations reveal novel interactions of the staples with the target protein. Cell Cycle. 2010; 9(22): 4560–4568. doi:doi: 10.4161/cc.9.22.13816 PMID: 21088491

35. Morrone JA, Perez A, Deng Q, Ha SN, Holloway MK, Sawyer TK, et al. Molecular simulations identify binding poses and approximate affinities of stapled α-helical peptides to MDM2 and MDMX. J Chem Theory Comput. 2017; 13(2): 863−869. doi:doi: 10.1021/acs.jctc.6b00978 PMID: 28042965